Effects of Fly Ash Loading on the Characteristics of PVC-based Cation Exchange Membranes for Reverse Electrodialysis

Heru Susanto[1,2*], Yunita Fahmi[1,2], Anisa Tri Hutami [1], Yuliyanto Triyono Hadi[1]

[1]Department of Chemical Engineering, Faculty of Engineering, Diponegoro University, Jl. Prof. Soedarto, Tembalang, Semarang 50275, Indonesia
[2]Membrane Research Center, Integrated Laboratory for Research and Services, Diponegoro University, Jl. Prof. Soedarto, Tembalang Semarang 50275, Indonesia

Abstract. This study investigated the effects of fly ash loading on the characteristics of polyvinyl chloride (PVC) membranes for reverse electrodialysis (RED). The membranes were prepared by adding different concentrations of fly ash (0.5–2 wt%) to the casting solution. The surface chemistry of the prepared membranes was analyzed using Fourier transform infrared spectroscopy. The swelling degree (SD) was used as an indicator of the membranes' water uptake. Titration using NaOH (0.01 M) was performed to measure the membranes' ion exchange capacity (IEC) and conductivity. The PVC membrane with 2 wt% fly ash demonstrated the highest SD (83.78%), IEC (0.163 meq/g), and conductivity (8.7×10^{-2} μS/cm). The results show that the presence of fly ash significantly affects the characteristics of PVC membranes for RED.

Keywords: Cation exchange membrane; Fly ash; Reverse electrodialysis

1. Introduction

Global energy scarcity has encouraged efforts to create renewable and sustainable energy (Setiawan et al., 2016). The use of such energy has also become crucial for the prevention of environmental problems. Recently, membrane-based gradient salinity has attracted considerable interest as a prospective renewable and sustainable energy source (Logan and Elimelech, 2015; NRC, 2015). Salinity gradient power can be defined as energy resulting from the mixture of two fluids with different salt concentrations, such as river water and seawater (Hong et al., 2015). The process of power generated through controlled mixing of fresh and salt water has not been explored as extensively as solar and wind power generation or other sustainable power generation methods (Gilstrap, 2013).

There are two methods for salinity difference–based energy generation, namely pressure-retarded osmosis and reverse electrodialysis (RED). In the past few years, researchers have focused on investigating RED for the desalination of river water and seawater (Post and Veerman, 2007). In 1954, Pattle established RED principles, proving that energy can be produced by mixing river water and seawater. Over the last decade, many studies on RED for energy generation were reported (Avci et al., 2018; Mei and Tang, 2018; Moreno et al., 2018; Ciofalo et al., 2019; Mehdizadeh et al., 2019). Lacey (1980) showed that to optimize energy production, membranes with good selectivity and low

resistance are required. Turek and Bandura (2007) reported that thin membranes with large contact   areas can improve energy production efficiency by shortening the ion flow pathways. Thereafter, efforts to produce membranes for RED have been proposed (Guler and Nijmeijer, 2018; Luo et al., 2018).

Improving the characteristics of ion exchange membranes through various modification techniques has received considerable attention. Sulfonation and carboxylation aim to supply negative charges to ion exchange membranes. Sulfonation is the most used method for the modification of membranes used in water filtration, dialysis diffusion, electrodialysis, and water cleavage. It is an electrophilic substitution process generally involving aromatic rings and increases membrane charge density, hydrophilicity, and conductivity. Sulfuric acid and chlorosulfate acid are commonly used as sulfonating agents (Hong et al., 2015).

Polyvinyl chloride (PVC) is a versatile thermoplastic polymer that shows appropriate chemical and biological resistances for water applications (Giwa et al., 2019). Inorganic nanoparticles are frequently incorporated into polymeric membrane matrixes to increase the membranes' performance, including functionality and thermal, chemical, and mechanical stability (Poerwadi et al., 2020). Developments in ion exchange membranes with the introduction of inorganic nanoparticles using aluminum oxide (Hosseini et al., 2012), titanium oxide (Nemati et al., 2015), and iron oxide (Hong and Chen, 2014) have been reported. However, most studies have used pure inorganic nanoparticles, which are either expensive or must be previously synthesized. Numerous inorganic nanoparticles are also available in nature, although their purity may be relatively low. Incorporating such nanoparticles into polymeric membrane matrixes is an interesting prospect.

Fly ash nanoparticles have attracted considerable interest due to their unique properties, including low density and cost and smooth spherical surfaces. More importantly, because fly ash is a coal combustion residue from thermal power plants, its use can offer environmental benefits. The main components of fly ash are oxides of silica, aluminum, iron, and calcium (Janani et al., 2018). Jin et al. (2012) found that the addition of nano-SiO_2 in the skin layer improved thermal stability and hydrophilicity and enhanced the nanofiltration membrane's permeation properties without rejection rate loss.

To the best of our knowledge, there is no research into the utilization of fly ash for fabricating ion exchange membranes. Therefore, this work aimed to study the effects of fly ash loading on the characteristics of membranes for RED. It was hypothesized that the presence of fly ash would improve the membranes' ion exchange characteristics.

2. Methods

2.1. Materials

Polyvinyl chloride (grade K-70) was donated by Asahimas Chemical Company, Indonesia. N-methyl pyrrolidine (NMP; grade ≥99.5%), NaCl (≥99%), sulfuric acid (96%), and NaOH (≥97%) were purchased from Merck, Germany. All chemicals were used without further purification. Water was purified with a homemade reverse osmosis–ion exchange unit. Fly ash was obtained from the Tanjung Jati B power plant, Jepara, Indonesia. Milling and screening (325 mesh sizes) were performed to obtain fly ash nanoparticles.

2.2. Membrane Preparation

For the preparation of polymeric membranes, phase inversion, which is induced by immersion–precipitation, was employed. Fly ash was dispersed in 83.5 mL of NMP. Then, 14 g of PVC was dissolved in the NMP–fly ash solution, which was stirred at room temperature for ~24 h to achieve homogeneity. The solution was then cast on glass support

with a 300-μm membrane thickness. Once it was created, it remained in a water immersion bath for 24 h and was then rinsed to remove the solvent. The characteristics of the prepared membranes are shown in Table 1.

Table 1 Composition of the casting solutions

Membrane	PVC (wt%)	Fly ash (wt%)
A	14	0.0
B	14	0.5
C	14	1.0
D	14	2.0

2.3. Posttreatment

PVC was sulfonated to introduce negatively charged groups into the polymer membranes. Sulfonation was performed using sulfuric acid at room temperature. Membrane sheets were cut with a circular punch 4 cm in diameter and dried in a desiccator for 6 h. The cation exchange membranes were immersed in 0.1 M H_2SO_4 at 60°C for 1 h and then in Aqua Dest at 80°C for 6 h to remove excessive H_2SO_4. Finally, they were cleaned with Aqua Dest until a neutral pH was reached.
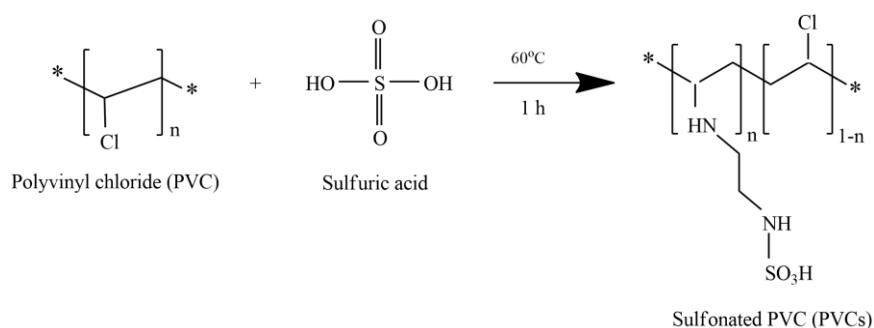
Figure 1 PVC sulfonation process

2.4. Membrane Characterizations

2.4.1. Surface chemistry

Fourier transform infrared (FTIR) spectroscopy was used to identify the functional groups on the membrane surfaces. The FTIR spectra of sulfonated and unsulfonated ion exchange membranes were determined using the Varian 3100 Excalibur FT-IR series, USA. The experiments were conducted using 64 scans at a resolution of 4 cm^{-1}.

2.4.2. Surface morphology

Scanning electron microscopy (JSM 6510 LA, JEOL, Japan) images were obtained to observe the morphological structures of the synthesized membranes. The outer surface of small membrane samples was sputtered with platinum for 30 s before the surface morphology was observed.

2.4.3. Swelling degree

The swelling degrees (SD) of the ion exchange membranes were measured using gravimetric methods. Membrane samples were immersed in NaCl solution for at least 24 h. They were then wiped using tissue paper and weighed to determine the wet membrane (swollen membrane) weight. They were subsequently dried at 50°C for 48 h and weighed to determine the dry weight. The SD was determined according to the following equation (Güler, 2014):

$$SD = \frac{W_{wet} - W_{dry}}{W_{dry}} \times 100\% \tag{1}$$

where W_{wet} (g) and W_{dry} (g) are the wet and dry membrane weights, respectively.

2.4.4. Ion exchange capacity

Ion exchange capacity (IEC) is defined as the number of active sites in an ion exchange membrane (Kumar et al., 2018). In this work, IEC was measured using a conventional titration method (Salarizadeh et al., 2017). Membrane samples were equilibrated in a saturated NaCl solution at room temperature for at least 48 h to induce the replacement of Na^+ with H^+ ions. The samples were then titrated with 0.01 M NaOH. The membranes' IEC was then determined by the following equation (Hong and Chen, 2014):

$$IEC = \frac{C_{NaOH} - V_{NaOH}}{W_{dry}} \qquad (2)$$

where C_{NaOH} represents the NaOH concentration (mol L^{-1}), V_{NaOH} is the volume of the NaOH solution (L), and W_{dry} is the membrane's dry weight (g).

2.4.5. Fixed charge density

Fixed charge density (FCD) describes the number of fixed charge groups in a given mass of water in the membrane. The FCD was determined as follows (Güler, 2014):

$$C_{fix} = \frac{IEC}{SD} \qquad (3)$$

where C_{fix} is the FCD (mmol/g of H_2O), IEC is the ion exchange capacity (mmol/g of dry membrane), and SD is the swelling degree (g of H_2O/g of dry membrane).

2.4.6. Membrane conductivity

An LCR meter (Krisbow, Indonesia) was used to measure the membranes' conductivity in σ (S/cm) with a frequency ranging from 42 Hz to 5 MHz. The membrane samples were equilibrated in deionized water for at least 24 h. Each sample was cut according to the size of the electrode used in the measurement cell. Membrane conductivity was then calculated using the following equation (Akli et al., 2016):
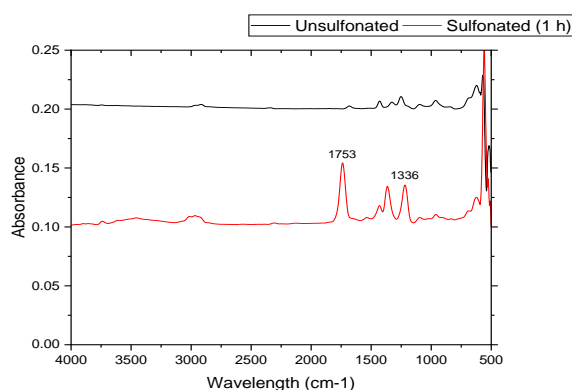
$$\sigma = \frac{L}{RA} \qquad (4)$$

where L is the distance between the electrodes, R is the resistance, and A is the cross-sectional area.

3. Results and Discussion

3.1. Modification by Sulfonation

The FTIR spectra of the PVC membranes are shown in Figure 2.

Figure 2 FTIR spectra of the PVC membranes

All spectra exhibited peaks in the region of 550–675 cm^{-1}. The peaks revealed the presence of C–Cl compounds. Infrared vibration bands characteristic of C=O stretching were observed between 1740 and 1780 cm^{-1}. Moreover, the prevalence of a strong band at the 1372–1335 cm^{-1} region indicated the presence of sulfonate groups (Kafle, 2020). An absorption band characteristic of SO$_2$ stretching at 1335 cm^{-1} was observed in the sulfonated membranes. This suggests that SO$_2$ groups had been introduced into the membranes through sulfonation. Peaks indicating the presence of sulfone groups were absent from the FTIR spectrum of the unsulfonated membrane. Overall, these results confirm that the PVC membranes were successfully sulfonated by immersion in a solution of 0.1 M sulfuric acid for 1 h.

3.2. Membrane Morphology

All membranes showed a porous structure within the range of macroporous materials. Sulfonation slightly reduced the pore sizes (Figures 3a and 3b). The presence of fly ash also decreased the pore size in both sulfonated and unsulfonated membranes (Figures 3c and 3d). No agglomeration of inorganic nanoparticles was observed in the membranes loaded with fly ash, indicating that it was well dispersed in the polymer membrane solution.
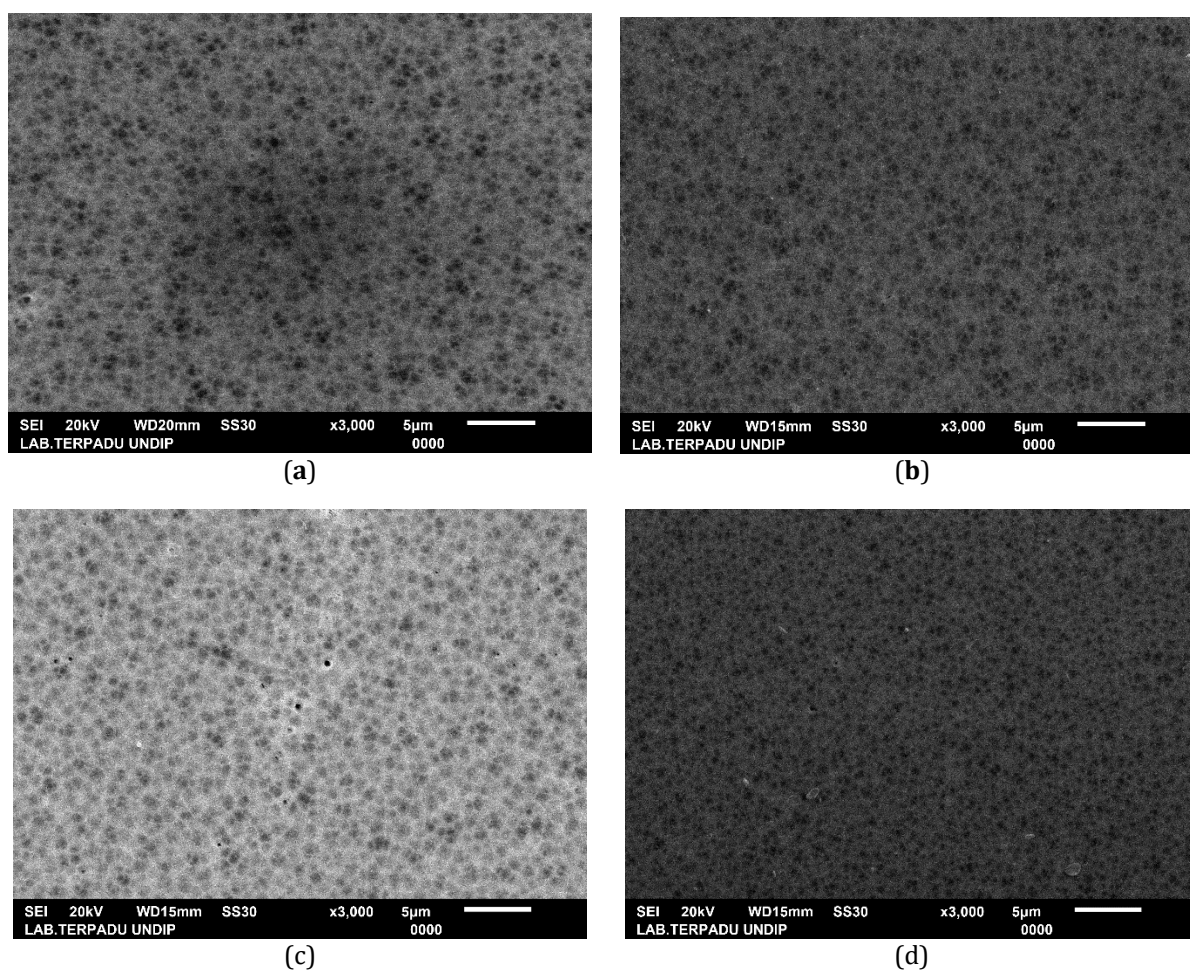
Figure 3 Membrane morphology structures: (a) 0 wt% fly ash without sulfonation; (b) 0 wt% fly ash with sulfonation; (c) 1 wt% fly ash without sulfonation; (d) 1 wt% fly ash with sulfonation

3.3. Effects of Fly Ash Loading on the Membranes' Swelling Degree
The membranes' SD is presented in Figure 4.
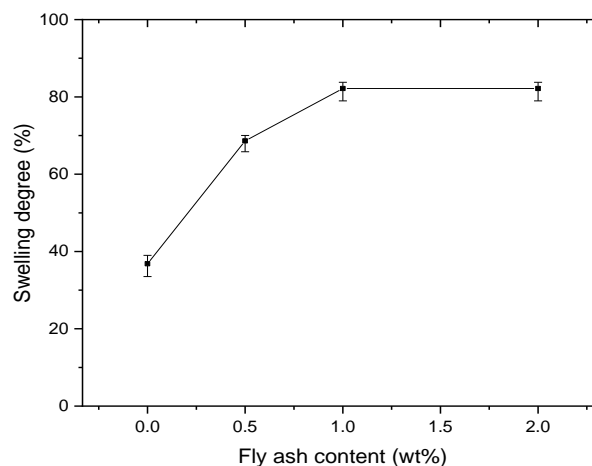
Figure 4 Swelling degree of the ion exchange membranes as a function of fly ash content

The addition of 1 wt% fly ash increased the membranes' SD. However, increasing the fly ash content to 3 wt% slightly decreased it. This can be explained as follows. The effect of nanoparticles on the membrane's SD is determined by their characteristics, including porosity or specific surface area and hydrophilicity. An increase in the porosity or specific surface area of nanoparticles increases the membrane's SD. On the other hand, if the nanoparticles are less hydrophilic than the polymer membrane material, they can decrease the membrane's SD. The addition of up to 1 wt% fly ash thus increased the membrane's specific surface area, whereas its hydrophobicity took hold in concentrations above 1 wt%. These phenomena have been observed in various nanoparticles (Swain et al., 2013; Nemati et al., 2015; Akli et al., 2016).

3.4. Effects of Fly Ash Loading on the Membranes' Ion Exchange Capacity
Figure 5 shows the effects of fly ash loading on the membranes' IEC.
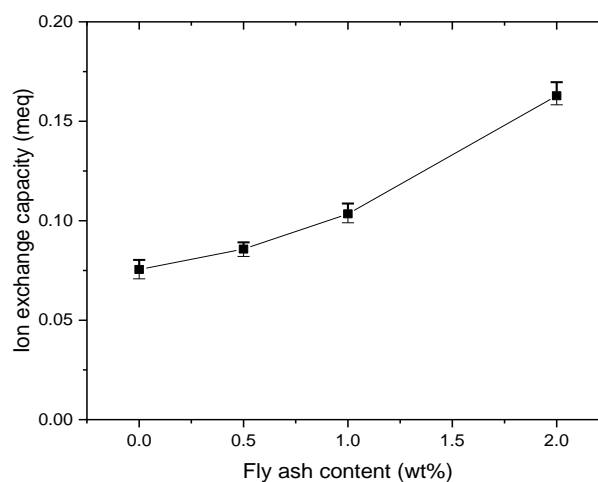
Figure 5 Ion exchange capacity of the PVC membranes as a function of fly ash content

The membranes' IEC increased as the fly ash content increased. The membrane with the highest fly ash content (2 wt%) yielded the highest IEC value (0.163 meq/g). Similar

results were obtained by Hosseini et al. (2012) in the preparation of cation exchange PVC membranes modified with iron–nickel nanoparticles. They reported that the addition of up to 2 wt% increased the IEC because the adsorption ability of iron–nickel oxide nanoparticles promoted interactions between ions and the membrane surface. This effect, in turn, facilitated ion transport between the membrane phase and the solution and promoted ion exchange. However, a further increase in the nanoparticle content reduced the IEC. It is important to note that we were unable to test membranes with more than 2 wt% fly ash, as this resulted in an inhomogeneous polymer solution, with fly ash forming clumps.

3.5. Effects of Fly Ash Loading on the Membranes' Fixed Charge Density
Figure 6 shows the membranes' FCD.
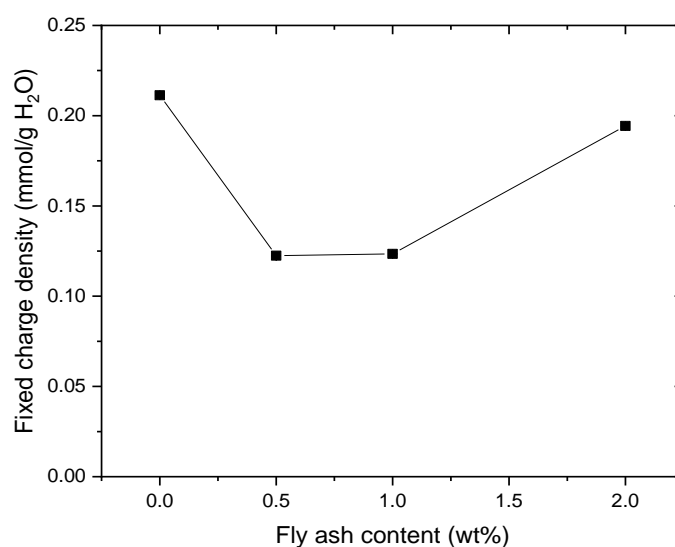
Figure 6 Fixed charge density of ion-exchange membranes as a function of fly ash content

The addition of fly ash initially decreased the fixed charge density of the PVC membranes. Increasing the fly ash content resulted in an increase in FCD; however, its value was still lower than that of the membrane without fly ash. The reason behind this phenomenon is that FCD was influenced by the membranes' IEC and SD. It increased with an increasing IEC, while it decreased with an increasing SD (Figures 4 and 5). A significant increase in FCD was thus obtained by increasing the fly ash content from 1 to 2 wt%, which did not increase the SD further, while it significantly increased the IEC.

3.6. Effects of Fly Ash Loading on the Membranes' Conductivity
Figure 7 shows that an increase in fly ash content in some cases increased and in others decreased the membrane conductivity. The conductivity of the PVC membranes with and without added fly ash was influenced by their chemical and physical characteristics. The minerals contained in fly ash increased conductivity, whereas an increase in porosity decreased it due to the higher air fraction in the membrane pores. The highest membrane conductivity (8.7×10^{-2} μS/cm) was observed in the membrane with 2 wt% fly ash.
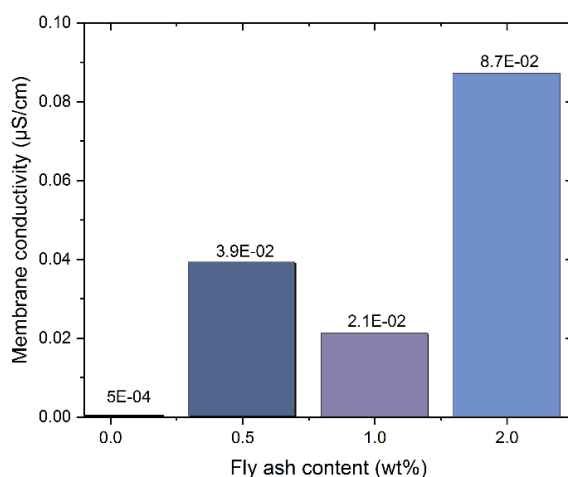
Figure 7 Conductivity of ion exchange membranes with different fly ash contents

4.   Conclusions

The composition of the polymer solution significantly influenced the membranes' properties. Membranes prepared with 2 wt% fly ash content showed the highest SD, IEC, and conductivity. It can thus be concluded that the addition and content of fly ash to PVC membrane solutions significantly affects the characteristics of PVC membranes for RED.

Acknowledgements

References

Akli, K., Supadi, K., Wenten, I.G., 2016. Preparation and Characterization of Heterogeneous PVC-Silica Proton Exchange Membrane. *Journal of Membrane Science and Research*, Volume 460, pp. 139–147

Avci, A.H., Tufa, R.A., Fontananova, E., Di Profio, G., Curcio, E., 2018. Reverse Electrodialysis for Energy Production from Natural River Water and Seawater. *Energy*, Volume 165(Part A), pp. 512–521

Ciofalo, M., La Cerva, M., Di Liberto, M., Gurreri, L., Cipollina, A., Micale, G., 2019. Optimization of net power density in Reverse Electrodialysis. *Energy*, Volume 181, pp. 576–588

Gilstrap, M.C., 2013. *Renewable Electricity Generation from Salinity Gradients using Reverse Electrodialysis.* Master's Thesis, Master of Science Program, Georgia Institute of Technology, Atlanta, GA, USA

Giwa, A., Ahmed, M., Hasan, S.W., 2019. Polymers for Membrane Filtration in Water Purification. *Polymeric Materials for Clean Water*, Das, R. (ed.), Springer, Cham, Switzerland, pp. 167–190

Güler, E., 2014. *Anion Exchange Membrane Design for Reverse Electrodialysis.* PhD Dissertation, Doctorate Program, University of Twente, Enschede, Netherlands

Guler, E., Nijmeijer, K., 2018. Reverse Electrodialysis for Salinity Gradient Power Generation: Challenges and Future Perspectives. *Journal of Membrane Science and Research*, Volume 4(3), pp. 108–110

Hong, J.G., Chen, Y., 2014. Nanocomposite Reverse Electrodialysis (RED) Ion-Exchange Membranes for Salinity Gradient Power Generation. *Journal of Membrane Science*, Volume 460, pp. 139–147

Hong, J.G., Zhang, B., Glabman, S., Uzal, N., Dou, X., Zhang, H., Chen, Y., 2015. Potential Ion-Exchange Membranes and System Performance in Reverse Electrodialysis for Power Generation: A Review. *Journal of Membrane Science*, Volume 486, pp. 71–88

Hosseini, S.M., Gholami, A., Madaeni, S.S., Moghadassi, A.R., Hamidi, A.R., 2012. Fabrication of (Polyvinyl Chloride/Cellulose Acetate) Electrodialysis Heterogeneous Cation Exchange Membrane: Characterization and Performance in Desalination Process. *Desalination*, Volume 306, pp. 51–59

Janani, S., Santhi, A.S., 2018. Multiple Linear Regression Model for Mechanical Properties and Impact Resistance of Concrete with Fly Ash and Hooked-end Steel Fibers. *International Journal of Technology*, Volume 9(3), pp. 526–536

Jin, L.M., Shi, W.X., Yu, S.L., Yi, X.S., Sun, N., Ma, C., 2012. Preparation and Characterization of a Novel PA-SiO$_2$ Nanofiltration Membrane for Raw Water Treatment. *Desalination*, Volume 298, pp. 34–41

Kafle, B.P., 2020. *Chemical Analysis and Material Characterization by Spectrophotometry*, Elsevier, Amsterdam, Netherlands

Kumar, P., Bharti, R.P., Kumar, V., Kundu, P.P., 2018. Polymer Electrolyte Membranes for Microbial Fuel Cells: Part A. Nafion-based Membranes. *Progress and Recent Trends in Microbial Fuel Cells*, Kundu P.P., Dutta, K. (eds.), Elsevier, Amsterdam, Netherlands, pp. 47–72

Lacey, R.E., 1980. Energy by Reverse Electrodialysis. *Ocean Engineering*, Volume 7(1), pp. 1–47

Logan, B.E., Elimelech, M., 2015. Membrane-based Processes for Sustainable Power Generation using Water. *Nature*, Volume 488, pp. 313–319

Luo, T., Abdu, S., Wessling, M., 2018. Selectivity of Ion Exchange Membranes: A Review. *Journal of Membrane Science*, Volume 555, pp. 429–454

Mehdizadeh, S., Yasukawa, M., Kuno, M., Kawabata, Y., Higa, M., 2019. Evaluation of Energy Harvesting from Discharged Solutions in a Salt Production Plant by Reverse Electrodialysis (RED). *Desalination*, Volume 467, pp. 95–102

Mei, Y., Tang, C.Y., 2018. Recent Developments and Future Perspectives of Reverse Electrodialysis Technology: A Review. *Desalination*, Volume 425, pp. 156–174

Moreno, J., Grasman, S., van Engelen, R., Nijmeijer, K., 2018. Upscaling Reverse Electrodialysis. *Environmental Science and Technology*, Volume 52, pp. 10856–10863

National Research Council (NRC), 2015. *Advancing the Science of Climate Change*, National Academy Press, Washington, D.C., USA

Nemati, M., Hosseini, S.M., Bagheripour, E., Madaeni, S.S., 2015. Electrodialysis Heterogeneous Anion Exchange Membranes Filled with TiO$_2$ Nanoparticles: Membranes' Fabrication and Characterization. *Journal of Membrane Science and Research*, Volume 1(3), pp. 135–140

Poerwadi, B., Kartikowati, C.W., Oktavian, R., Novareza, O., 2020. Manufacture of a Hydrophobic Silica Nanoparticle Composite Membrane for Oil-Water Emulsion Separation. *International Journal of Technology*, Volume 11(2), pp. 364–373

Post, J.W., Veerman J., 2007. Salinity-Gradient Power: Evaluation of Pressure-Retarded Osmosis and Reverse Electrodialysis. *Journal of Membrane Science*, Volume 288(1–2), pp. 218–230

Salarizadeh, P., Javanbakht, M., Pourmahdian, S., 2017. Enhancing the Performance of SPEEK Polymer Electrolyte Membranes using Functionalized TiO_2 Nanoparticles with Proton Hopping Sites. *RSC Advances*, Volume 7, pp. 8303–8313

Setiawan, E.A., Asvial, M., 2016. Renewable Energy's Role in a Changing World. *International Journal of Technology*, Volume 7(8), pp. 1280–1282

Swain, S., Sharma, R., Bhattacharya, S., Chaudhari, L., 2013. Effects of Nano-Silica/Nano-Alumina on Mechanical and Physical Properties of Polyurethane Composites and Coatings. *Transactions on Electrical and Electronic Materials*, Volume 14(1), pp. 1–8

Turek, M., Bandura, B., 2007. Renewable Energy by Reverse Electrodialysis. *Desalination*, Volume 205(1), pp. 67–74